Dalton Transactions

PAPER

View Article Online
View Journal | View Issue



Cite this: *Dalton Trans.*, 2014, **43**, 14302

# Catalytic bond forming reactions promoted by amidinate, guanidinate and phosphaguanidinate compounds of magnesium†

Ryan J. Schwamm,[a] Benjamin M. Day,[b] Natalie E. Mansfield,[b] William Knowelden,[b] Peter B. Hitchcock[b] and Martyn P. Coles*[a]

Received 14th April 2014,
Accepted 7th May 2014

DOI: 10.1039/c4dt01097c

www.rsc.org/dalton

The synthesis and catalytic properties of a series of magnesium compounds consisting of monoanionic, *N*,*N*′-chelating ligands (NnN = amidinates, guanidinates, phosphaguanidinates) is reported. The compounds were synthesized by (i) insertion of a carbodiimide into an existing Mg–C or Mg–N bond, or (ii) protonolysis of an organomagnesium compound by a neutral pre-ligand. Structural analyses of *mono*- or bis-(chelate) compounds with general formula Mg(NnN)X(L)$_n$ and Mg(NnN)$_2$(L)$_n$ (X = halide, aryloxide, amide; L = Et$_2$O, THF; $n$ = 0, 1 or 2) have been performed and the influence that the ligand substituent patterns have on the solid-state structures has been probed. Selected examples of the compounds were tested as (pre)catalysts for the polymerization of lactide, the dimerization of aldehydes and the hydroacetylenation of carbodiimides.

## Introduction

The application of group 2 compounds containing Mg, Ca, Sr, Ba as catalysts is an attractive area of research due to the relatively low toxicity of the metal and abundance of cheap/easily synthesised starting materials.[1–4] Magnesium is particularly favoured in this respect due to the ubiquitous presence of organomagnesium compounds in synthetic chemistry laboratories, typically in the form of Grignard reagents. Accordingly, in the last 5 years magnesium complexes have been reported for their activity as catalysts in a range of chemical transformations including hydroamination,[5–9] hydroboration,[10–13] cross-dehydrocoupling,[14] ring-opening polymerization (ROP),[15–17] and the homocoupling of aldehydes[18,19] (the Tishchenko reaction).[20] We have recently explored a series of magnesium amidinate and guanidinate compounds as (pre)-catalysts in selected bond forming reactions.[21–23] In this contribution we report additional results towards understanding the complex equilibrium chemistry involved in these catalytic cycles and the application of selected examples to ROP catalysis. To supplement the results from existing amidinate and guanidinate compounds, we have extended this area to include phosphaguanidinate compounds in which the carbon atom of the metallacycle is bonded to a –PR$_2$ substituent (Fig. 1). The structural consequences of the different substitution patterns are investigated for a range of four-, five- and six-coordinate compounds.

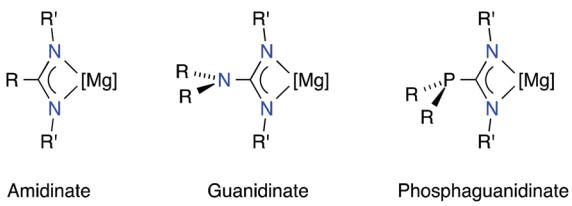


**Fig. 1** Generic amidinate, guanidinate and phosphaguanidinate ligands.

## Experimental

### General information

All manipulations were carried out under dry nitrogen using standard Schlenk-line and cannula techniques, or in a conventional nitrogen-filled glovebox. Solvents were dried over appropriate drying agents and degassed prior to use. All compounds were purchased from Sigma-Aldrich and used as received unless otherwise stated. MgMeCl (3 M solution in THF) and MgMeBr (3 M solution in Et$_2$O) were received as solutions. LiN{SiMe$_3$}$_2$ and KN{SiMe$_3$}$_2$ were crystallized from toluene; benzaldehyde was freshly distilled and stored under nitrogen; *rac*-Lactide was sublimed before use. Ph$_2$PC{NCy}{NHCy},[24] Cy$_2$PC

[a]*School of Chemical and Physical Sciences, Victoria University of Wellington, Wellington, 6012, New Zealand. E-mail: martyn.coles@vuw.ac.nz*
[b]*Department of Chemistry, University of Sussex, Falmer, Brighton BN1 9QJ, UK*
†Electronic supplementary information (ESI) available: Thermal ellipsoid plots of [**7**]$_2$, [**8**]$_2$ and **14**. CCDC 996734–996740. For ESI and crystallographic data in CIF or other electronic format see DOI: 10.1039/c4dt01097c

{N$^i$Pr}{NH$^i$Pr},[25] and Cy$_2$PC{NCy}{NHCy}[25] were synthesised as reported.

NMR spectra were recorded using a Bruker Avance DPX 300 MHz spectrometer at 300.1 ($^1$H), 75.4 ($^{13}$C{$^1$H}) and 121.5 ($^{31}$P{$^1$H}) MHz, a Varian INOVA system at 300.1 ($^1$H) or 75.3 ($^{13}$C{$^1$H}) MHz, or a Varian VNMR 400 MHz spectrometer at 400.1 ($^1$H), 100.3 ($^{13}$C{$^1$H}) and 161.9 ($^{31}$P{$^1$H}) MHz. Proton and carbon chemical shifts were referenced internally to residual solvent resonances; phosphorus chemical shifts were referenced to external $H_3PO_4$ (85% aq.). Coupling constants are quoted in Hz. Elemental analyses were performed by S. Boyer at London Metropolitan University.

**Synthesis of Mg(Ph$_2$PC{NCy}$_2$)Cl(THF) (6).** A solution of MgMeCl (0.08 mL of a 3 M solution in THF, 0.25 mmol) was added drop wise to a solution of Ph$_2$PC(NCy)(NHCy) (0.100 g, 0.25 mmol) in toluene. The resultant clear, colourless solution was stirred at ambient temperature for 16 hours prior to removal of volatiles under reduced pressure. Crystallization of the crude white solid by slow cooling a hot hexane solution to ambient temperature afforded **6** as colourless crystals. Yield 0.11 g (84%). Anal. Calcd for $C_{29}H_{40}N_2OMgPCl$ (523.37): C, 66.55; H, 7.70; N, 5.35%. Found: C, 66.49; H, 7.65; N, 5.33%. $^1$H NMR (300 MHz, $C_6D_6$): $\delta$ 7.74 (d t, $^3J_{HH}$ = 6.4, $^4J_{PH}$ = 1.5, 4H, *m*-C$_6H_5$), 7.54 (t, $^3J_{HH}$ = 6.1, 4H, *o*-C$_6H_5$), 7.12–7.02 (m, 2H, *p*-C$_6H_5$), 4.23 (m, 2H, Cy–$H_\alpha$), 4.12 (m, 4H, THF), 1.90–0.82 (m, 20H, Cy–C$H_2$), 1.47 (m, 4H, THF). $^{13}$C{$^1$H} NMR (75 MHz, $C_6D_6$): $\delta$ 170.8 (d, $^1J_{PC}$ = 53, P*C*N$_2$), 134.3 (d, $J_{PC}$ = 20, *C*$_6$H$_5$), 132.4 (d, $J_{PC}$ = 19, *C*$_6$H$_5$), 129.3 (*C*$_6$H$_5$), 129.0 (d, $J_{PC}$ = 7, *C*$_6$H$_5$), 69.4 (THF), 56.4 (d, $^3J_{PC}$ = 18, Cy–$C_\alpha$), 37.0, 35.7 (Cy–*C*H$_2$), 26.3 (THF), 25.2 (Cy–*C*H$_2$). $^{31}$P{$^1$H} NMR (121 MHz, $C_6D_6$): $\delta$ −23.6.

**Synthesis of Mg(Cy$_2$PC{NCy}$_2$)Br(OEt$_2$) (7).** The compound was made in an analogous manner to that described for **6**, using 0.22 mL of a 3 M solution of MgMeBr in Et$_2$O (0.66 mmol) and 0.250 g Cy$_2$PC{NCy}{NHCy} (0.64 mmol), and Et$_2$O as the solvent. Prolonged storage at 5 °C afforded a small number of colourless crystals (0.037 g, 10%) that were isolated and analysed by X-ray diffraction and elemental analysis. Anal. Calcd for $C_{29}H_{54}N_2OMgPBr$ (581.93): C, 59.85; H, 9.35; N, 4.81%. Found: C, 59.71; H, 9.57; N, 4.72%.

**Synthesis of Mg(Cy$_2$PC{N$^i$Pr}$_2$)Cl(THF) (8).** The compound was made in an analogous manner to that described for **6**, using 0.11 mL of a 3 M solution of MgMeCl in THF (0.33 mmol) and 0.100 g Cy$_2$PC{N$^i$Pr}{NH$^i$Pr} (0.31 mmol) in toluene. Crystallization from hot hexane afforded **8** as colourless crystals. Yield 0.09 g (60%). Despite repeated attempts, accurate elemental could not be obtained. $^1$H NMR (300 MHz, $C_6D_6$): $\delta$ 4.86 (m, 2H, C*H*Me$_2$), 4.80 (m, 2H, Cy–$H_\alpha$), 3.90 (m, 4H, THF), 2.33–0.82 (m, Cy–C$H_2$*), 1.43 (m, 4H, THF), 1.20 (d, $^3J_{HH}$ = 6.3, 12H, CH*Me*$_2$) [*total integral for cyclohexyl methylene groups = 20H]. $^{13}$C{$^1$H} NMR (75 MHz, $C_6D_6$): $\delta$ 170.8 (d, $J$ = 53, P*C*N$_2$), 68.6 (THF), 50.6 (d, $J$ = 18, Cy–$C_\alpha$), 46.9 (d, $J$ = 14, *C*HMe$_2$), 34.2 (d, $J$ = 17, Cy–*C*H$_2$), 32.6 (d, $J$ = 23, Cy–*C*H$_2$), 30.6 (d, $J$ = 12, Cy–*C*H$_2$), 26.4 (d, $J$ = 21, Cy–*C*H$_2$), 25.8 (s, CH*Me*$_2$), 25.6 (THF). $^{31}$P{$^1$H} NMR (121 MHz, $C_6D_6$): $\delta$ −9.9.

**Synthesis of Mg(Ph$_2$PC{NCy}$_2$)(OAr′)(THF) (12) (Ar′ = 2,6-$^t$Bu$_2$-4-MeC$_6$H$_2$).** A solution of MgMeCl (0.16 mL of a 3 M solution in THF, 0.48 mmol) was added drop wise to a clear colourless solution of Ph$_2$PC{NCy}{NHCy} (0.200 g, 0.50 mmol) in THF (~10 mL). The resultant clear, colourless solution was stirred at ambient temperature for 1 h before being added to a clear colourless solution of LiOAr′ (0.113 g, 0.50 mmol) in THF (~10 mL). Stirring for 16 h at ambient temperature followed by removal of volatiles *in vacuo* afforded a crude white solid. Extraction from LiCl with hot hexane and slow cooling to ambient temperature yielded colourless crystals of **12**. Yield 0.170 g (48%). Anal. Calcd for $C_{44}H_{63}N_2O_2MgP$ (707.26): C, 74.72; H, 8.98; N, 3.96%. Found: C, 74.66; H, 8.88; N, 3.99%. $^1$H NMR (300 MHz, $C_6D_6$): $\delta$ 7.66 (d t, $^3J_{HH}$ = 7.1, $^4J_{PH}$ = 1.5, 4H, *m*-C$_6H_5$), 7.32 (s, 2H, *m*-C$_6H_2$), 7.12–7.02 (m, 6H, *o*,*p*-C$_6H_5$), 3.82 (m, 2H, Cy–$H_\alpha$), 3.60 (m, 4H, THF), 2.46 (s, 3H, Ar′–C$H_3$), 1.83 (s, 18H, Ar′–C(C$H_3$)$_3$, 1.68–1.00 (m, 20H, Cy–C$H_2$), 1.17 (m, 4H, THF). $^{13}$C{$^1$H} NMR (75 MHz, $C_6D_6$): $\delta$ 172.5 (d, $^1J_{PC}$ = 49, P*C*N$_2$), 160.9 (s, *i*-*C*$_6$H$_2$), 137.2 (*C*$_6$H$_2$), 135.5 (d, $J_{PC}$ = 17, *C*$_6$H$_5$), 134.3 (d, $J_{PC}$ = 19, *C*$_6$H$_5$), 132.3 (d, $J_{PC}$ = 19, *C*$_6$H$_5$), 129.1 (*C*$_6$H$_2$), 125.7 (*C*$_6$H$_2$), 121.3 (*C*$_6$H$_2$), 69.6 (THF), 56.0 (d, $^3J_{PC}$ = 18, Cy–$C_\alpha$), 37.2, 35.6 (Cy–*C*H$_2$), 31.8 (Ar′–C(*C*H$_3$)$_3$), 26.2 (THF), 24.9 (Cy–*C*H$_2$), 21.7 (Ar′–*C*H$_3$). The resonance for *C*(CH$_3$)$_3$ could not be confidently assigned due to it's low intensity and possible overlap with other signals. $^{31}$P{$^1$H} NMR (121 MHz, $C_6D_6$): $\delta$ −20.5.

**Synthesis of Mg(Ph$_2$PC{NCy}$_2$)(N{SiMe$_3$}$_2$)(THF) (14).** A solution of MgMeCl (0.16 mL of a 3 M solution in THF, 0.48 mmol) was added drop wise to a clear colourless solution of Ph$_2$PC{NCy}{NHCy} (0.200 g, 0.50 mmol) in THF (~10 mL). The resultant clear, colourless solution was stirred at ambient temperature for 1 h before being added to a solution of KN{SiMe$_3$}$_2$ (0.100 g, 0.50 mmol) in THF (~10 mL). Stirring for 16 h at ambient temperature followed by removal of volatiles *in vacuo* afforded a crude white solid. Extraction from the KCl with hot hexane with slow cooling to ambient temperature yielded colourless crystals of **14**. Yield 0.240 g (74%). Anal. Calcd for $C_{35}H_{58}N_3OMgSi_2P$ (648.30): C, 64.84; H, 9.02; N, 6.48%. Found: C, 64.88; H, 9.02; N, 6.55%. $^1$H NMR (300 MHz, $C_6D_6$): $\delta$ 7.67 (d t, $^3J_{HH}$ = 8.4, $^4J_{PH}$ = 1.3, 4H, *m*-C$_6H_5$), 7.10 (t, $^3J_{HH}$ = 6.2, 4H, *o*-C$_6H_5$), 7.02 (t, $J$ = 5.1, 6H, *p*-C$_6H_5$), 3.79 (m, 2H, Cy–$H_\alpha$), 3.68 (m, 4H, THF), 1.60–1.00 (m, 20H, Cy–C$H_2$), 1.26 (m, 4H, THF), 0.48 (s, 18H, Si*Me*$_3$). $^{13}$C{$^1$H} NMR (75 MHz, $C_6D_5$): $\delta$ 171.9 (d, $^1J_{PC}$ = 48, P*C*N$_2$), 135.7 (d, $J_{PC}$ = 17, *C*$_6$H$_5$), 132.3 (d, $J_{PC}$ = 18, *C*$_6$H$_5$), 128.7 (*C*$_6$H$_5$), 68.8 (THF), 56.2 (d, $^3J_{PC}$ = 18, Cy–$C_\alpha$), 37.5 (Cy–*C*H$_2$), 26.2 (THF), 26.1, 25.1 (Cy–*C*H$_2$), 6.3 (Si*Me*$_3$). $^{31}$P{$^1$H} NMR (121 MHz, $C_6D_6$): $\delta$ −20.7.

**Synthesis of Mg(Cy$_2$PC{NCy}$_2$)(N{SiMe$_3$}$_2$)(THF) (15).** The compound was made in an analogous manner to that described for **14**, using 0.60 mL of a 3 M solution of MgMeBr in Et$_2$O (1.80 mmol), 0.730 g Cy$_2$PC{NCy}{NHCy} (1.80 mmol) and 0.300 g LiN{SiMe$_3$}$_2$ (1.80 mmol). Stirring for 18 h at ambient temperature followed by removal of volatiles *in vacuo* afforded a crude white solid. Extraction from LiCl with hot hexane and slow cooling to ambient temperature yielded colourless crystals of **15**. Yield 1.00 g (84%). Anal. Calcd for $C_{35}H_{70}N_3OMgSi_2P$ (660.40): C, 63.65; H, 10.68; N, 6.36%. Found: C, 63.51; H, 10.53; N, 6.26%. $^1$H NMR (400 MHz,

$C_6D_6$): $\delta$ 3.71 (m, 4H, THF), 2.30 (m, 2H, $Cy_{(P)}$–$H_\alpha$), 2.11–1.11 (m, 42H, $Cy_{(N)}$–$H_\alpha$ + $Cy_{(N/P)}$–$CH_2$), 1.27 (m, 4H, THF), 0.46 (s, 18H, Si$Me_3$). $^{13}C\{^1H\}$ NMR (100 MHz, $C_6D_6$): $\delta$ 174.8 (d, $^1J_{PC}$ = 49.7, P$CN_2$), 68.7 (THF), 38.0 (br), 36.0 (d, $^2J_{PC}$ = 18, $Cy_{(P)}$–$C_\alpha$), 33.5 (d, $J_{PC}$ = 23, $Cy_{(P)}$–$CH_2$), 32.0 (d, $J_{PC}$ = 12, $Cy_{(P)}$–$CH_2$), 27.4 (d, $J_P$ = 21, $Cy_{(P)}$–$CH_2$), 27.4, 26.6, 26.5 ($Cy_{(N)}$–$CH_2$), 25.2 (THF), 6.6 (Si$Me_3$). $^{31}P\{^1H\}$ NMR (161 MHz, $C_6D_6$): $\delta$ −8.3.

### Catalysis (typical procedures)

**Lactide polymerization.** A $C_6D_6$ solution of the pre-catalyst (0.01 mmol) and 20 equiv. *rac*-Lactide were combined in an NMR tube fitted with a J. Young's tap. NMR spectra were acquired after 10 minutes and then at 30 minute intervals.

**Dimerization of aldehydes.** An NMR tube fitted with a J. Young's tap was charged with 1 mol% of pre-catalyst followed by the addition of 0.5 mL of a $C_6D_6$ solution of 1,4-dimethoxybenzene (0.11 M). The NMR instrument was locked and shimmed to this sample and an experiment set up to record $^1$H NMR spectra (1 scan every 30 seconds) for the duration of the experiment. 0.1 mL of a $C_6D_6$ solution of benzaldehyde (4.77 M) was added to the sample in the glovebox. The experiment was started as soon as the sample was in the probe (maximum time elapsed after mixing = 2 minutes).

**Hydroacetylenation.** A solution of the magnesium compound in $C_6D_6$ (0.5 mL of a 0.0034 M standard solution, 1.7 μmol) was added to an NMR tube fitted with a J. Young's tap that had been previously charged with a mixture of phenyl acetylene (0.022 mL, 0.17 mmol) and *N*,*N*′-diisopropylcarbodiimide (0.028 mL, 0.17 mmol). The NMR tube was heated to 80 °C for 24 h with regular monitoring of the progress of the catalysis using $^1$H NMR spectroscopy. Yields of the propargylamidine were determined using peaks corresponding to the THF from **1** as an internal standard.

### Crystallography

Crystals were covered in inert oil and suitable single crystals were selected under a microscope and mounted on a Bruker AXS diffractometer (**15**) or an Enraf Nonius Kappa CCD diffractometer ([**6**]$_2$, [**7**]$_2$, [**8**]$_2$, **12** and **14**). Data were collected at 173(2) K using Mo Kα radiation at 0.71073 Å. The structures were refined with SHELXL-97.[26] Additional points are summarized below:

**[Mg(Cy$_2$PC{NCy}$_2$)Br(Et$_2$O)]$_2$ [7]$_2$.** The coordinated ether molecule was disordered and was modelled over two positions with C–C distances restrained to be equal.

**Mg(Ph$_2$PC{NCy}$_2$)(OAr′)(THF) 12.** The carbon atoms of the THF molecule were disordered over two positions and were modelled isotropically.

**Mg(Cy$_2$PC{NCy}$_2$)(N{SiMe$_3$}$_2$)(THF) 15.** There are two essentially identical molecules in the unit cell. One of the Si$Me_3$ groups is disordered over two positions; the carbon atoms of the lower occupancy position are modeled isotropically.

**Mg(*p*-tolC{NCy}$_2$)$_2$(THF)$_2$.** One cyclohexyl group and the coordinated THF group are disordered with the two components required to have the SAME geometry. For the THF solvate it was impossible to distinguish the position of the oxygen atom and all atom sites were set at 80% carbon, 20% oxygen; in addition there was conformational disorder of the solvate. All disordered atoms were left isotropic.

## Results and discussion

### Synthesis

The synthesis of magnesium compounds incorporating the *N*,*N*′-chelating ligands described in this study was achieved using two approaches. The insertion of carbodiimides into Mg–X bonds (Scheme 1) represents an atom efficient method for the preparation of amidinates (X = alkyl, aryl)[27–29] and guanidinates (X = amide).[27] We have used this route to access magnesium compounds with the [mesC{NCy}$_2$]$^-$ amidinate ligand (mes = 2,4,6-$Me_3C_6H_2$),[22] isolating bromide **1** as a pre-cursor to further derivation. We have also demonstrated that insertion into the Mg–N bonds of Mg(N{SiMe$_3$}$_2$)$_2$ affords the bis(guanidinate) compound Mg[(Me$_3$Si)$_2$NC{N$^i$Pr}$_2$]$_2$(THF) (**2**).[23]

Alternatively, the [N∩N]$^-$ ligand may be introduced to magnesium using a protonolysis methodology, employing the neutral amidine/guanidine and a suitable organo- or amido-magnesium reagent (Scheme 2).[28,30–36] We have used this route to prepare compounds incorporating the bicyclic guanidinates derived from 1,3,4,6,7,8-hexahydro-2*H*-pyrimido[1,2-*a*]-pyrimidine (hppH) and 1,4,6-triazabicyclo[3.3.0]oct-4-ene (Htbo).[21] However rather than give the expected Mg(N∩N)X(L)$_n$ compounds, the solid-state structures showed a preference for these ligands to adopt a bridging coordination mode (**3** and **4**, Fig. 2);[37] a similar coordination of the [hpp]$^-$ anion was observed in the tetrameric base-free compound [Mg(hpp)Br]$_4$ isolated in low yield by Himmel and co-workers.[30] We have used this approach to furnish the *mono*- and bis-(chelate) compounds **5** and **9** that incorporate the ethynylamidinate ligand [PhC≡CC{N$^i$Pr}$_2$]$^-$.[23]

We note that when attempting to isolate heteroleptic compounds of the type Mg(N∩N)X(L)$_n$ (X = halide), ligand redistribution can occur affording the bis(chelate) species, Mg(N∩N)$_2$(L)$_n$ with concomitant formation of $MgX_2(L)_n$.[31] Very minor changes to the ligand substituents can influence this process, illustrated by the contrasting results obtained from the insertion reaction of dicyclohexylcarbodiimide and THF

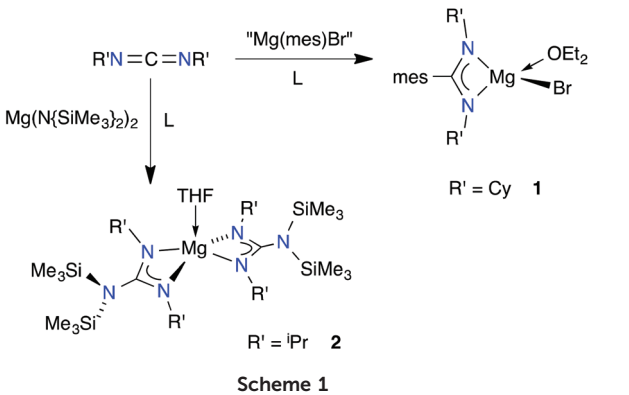


Scheme 1

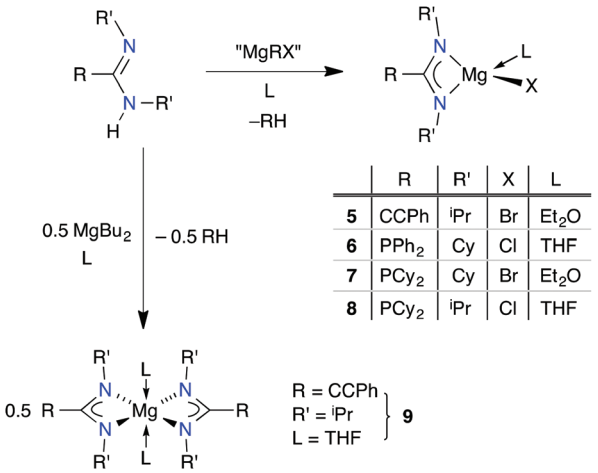


| | R | R' | X | L |
|---|---|---|---|---|
| 5 | CCPh | $^i$Pr | Br | $Et_2O$ |
| 6 | $PPh_2$ | Cy | Cl | THF |
| 7 | $PCy_2$ | Cy | Br | $Et_2O$ |
| 8 | $PCy_2$ | $^i$Pr | Cl | THF |

Scheme 2

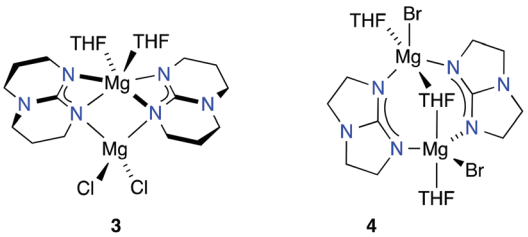


Fig. 2 Solid-state structure of **3** and **4**, showing bridging coordination of the guanidinate ligands.

solutions of MgRBr (R = mes, *p*-tolyl). In the former case the desired compound Mg(mesC{NCy}$_2$)Br(THF) (**1**) crystallized in good yield as the μ,μ-dibromo-bridged dimer. However, a reduction in bulk at the 2,6-positions of the arylmagnesium reagent afforded the solvated homoleptic products upon work-up, with fractional crystallization of Mg(*p*-tolylC{NCy}$_2$)$_2$(THF)$_2$‡ and $MgBr_2(THF)_4$. A similar ligand redistribution was exploited in this work to enable isolation of the bis(amidinate) species Mg(mesC{NCy}$_2$)$_2$(THF) (**10**), from the mixed amidinate/acetylide species **A** (Scheme 3).

We have used the protonolysis route to synthesize a series of phosphaguanidinate magnesium compounds from the reaction of the neutral species $Ph_2PC\{NCy\}\{NHCy\}$,[24] and $Cy_2PC\{NR'\}\{NHR'\}$ (R' = $^i$Pr, Cy),[25] with MgMeX (X = Cl, Br) solutions (**6–8**, Scheme 2). This approach was used rather than the carbodiimide insertion route that has successfully been employed by Hill[38,39] and Westerhausen[40] to synthesize phosphaguanidinate compounds of Ca, Sr and Ba, primarily due to the lack of availability of suitable magnesium phosphanides.[41]

Compounds **6** and **8** were isolated in good yield and characterized by $^1$H, $^{13}$C and $^{31}$P NMR spectroscopy. The yield for compound **7** was not optimized and spectroscopic data were

‡The composition of the amidinate species Mg(*p*-tolylC{NCy}$_2$)$_2$(THF)$_2$ was confirmed by X-ray diffraction (Fig. S4†) and the cif-file has been uploaded as a part of this contribution; no additional analytical data were obtained on this compound.

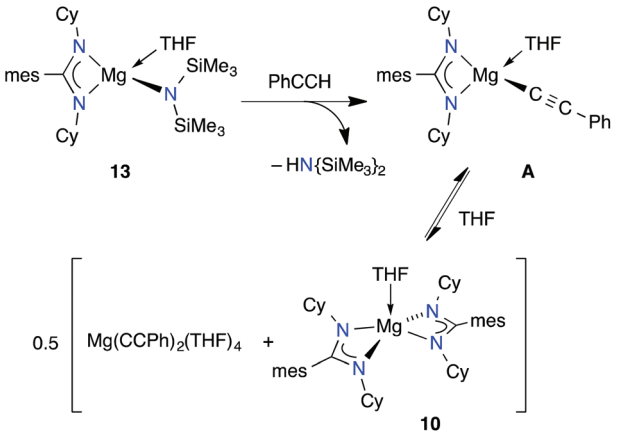


Scheme 3

not obtained; subsequent reactions generated this compound *in situ*. The $^1$H NMR of **6** and **8** were consistent with a symmetrically bound phosphaguanidinate ligand with a single bound THF molecule. The $^{31}P\{^1H\}$ NMR of diphenylphosphaguanidinate derivative **6** shows a singlet at $\delta_p$ −23.6, consistent with this ligand in the *N*,*N*'-chelated bonding mode ($\delta_p$ range: −17.3 to −23.8).[38–40,42–47] Similarly, the chemical shift for the $Cy_2P$-derivative, **8** ($\delta_p$ −9.9) is consistent with other *N*,*N*'-chelated ligands incorporating this substitution at phosphorus ($\delta_p$ range: −7.4 to −11.0).[44]

Metathesis reactions of the Mg(N∩N)X(L)$_n$ compounds has been successfully performed using MOAr (M = Li, K; Ar = 2,6-$^t$Bu$_2$C$_6$H$_3$, 2,6-$^t$Bu$_2$-4-MeC$_6$H$_2$) and MN{SiMe$_3$}$_2$ (M = Li, K) to access aryloxide (**11** and **12**) and bis(trimethylsilyl)amide derivatives **13–15** (Scheme 4). The $^1$H NMR spectrum of each compound was consistent with a symmetric *N*,*N*'-chelated ligand, with a single THF at the metal. The $^{31}P\{^1H\}$ NMR chemical shifts for the phosphaguanidinate derivatives vary according to the phosphorus substituents, as reported above, with no significant difference observed between the aryloxide **12** ($\delta_p$ −20.5) and the amide **14** ($\delta_p$ −20.7) of the 'Mg($Ph_2PC\{NCy\}_2$)(THF)' fragment. The presence of THF was not indicated in the NMR spectra of the hpp-amide compound Mg(hpp)(N{SiMe$_3$}$_2$) **16**, and the corresponding [tbo]$^-$ compound

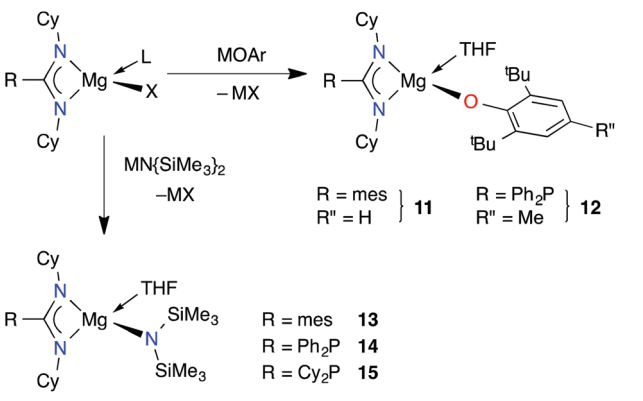


Scheme 4

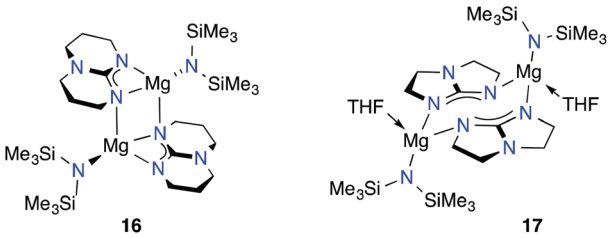


Fig. 3 Solid-state structure of **16** and **17**.

**17** showed a guanidinate : amide : THF ratio of 1 : 1 : 1.[21] The solid-state structures of these compounds showed bridging ligands, as observed in **3** and **4** (Fig. 3).

## Structural study

X-ray diffraction analysis has been performed on phosphaguanidinate compounds **6–8**, **12**, **14** and **15** (Tables 1–5). The results are presented alongside selected examples from our previous work.

As observed in related amidinate[48] (including **1**),[22] and guanidinate[32,49] compounds, the Mg(R$_2$PC{NR′}$_2$)X(L) complexes crystallize as the μ,μ-dihalobridged dimers with chelating [N∩N]$^-$ ligands (Fig. 4 for [**6**]$_2$; Fig. S1 and S2† for [**7**]$_2$ and [**8**]$_2$: see ESI†). The magnesium centres are five-coordinate with the remaining site occupied by an *O*-bound ether molecule (THF or Et$_2$O). The resultant geometries are best described as distorted square-based pyramidal in which the apical position is occupied by the ether oxygen atom, with $\tau_5$-values[50] between 0.30 and 0.40. In contrast, the amidinate structure [**1**]$_2$ has a $\tau_5$-value of 0.70 and may therefore be considered as a distorted trigonal bipyramid, with N1 and Br′ defining the apical positions. This change in geometry arises mainly from an increased twisting of the plane of the metallacycle relative to the plane defined by N1–Mg–O, such that the N2–Mg–X angle is considerably less in the amidinate than in the phosphaguanidinate (123.66(8)° and 144.36(6)°, respectively, Fig. 5). The $\tau_5$-values of 0.56 and 0.48 for the two independent magnesium centres in propargylamidinate derivative [**5**]$_2$ illustrate that this is a relatively 'soft' parameter that can be influenced strongly by subtle changes in the ligand. Overall it appears that there is no clear preference for either trigonal bipyramidal or square-based pyramidal metal geometry in compounds that adopt this general structure type.

Despite a tendency towards asymmetry in the Mg–N bonds (range $\Delta_{MgN}$: 0.025 Å to 0.078 Å), consistent with inequivalent axial and equatorial (or basal and apical) positions for each of the idealized five-coordinate geometries, the C–N bond lengths within the metallacycle are indistinguishable (within 3$\sigma$). This is consistent with symmetric delocalization of π-electron density in the heteroallylic unit. The bite angle of the ligand is largely invariant of the substitution pattern (range 63.93(12)° to 64.76(8)°) suggesting a robust MgN$_2$C metallacycle. The sum of angles at phosphorus (range $\sum_{angles}$(P): 309.5° to 311.3°) varies little between the Ph$_2$P- and Cy$_2$P-ligands, and indicates the availability of *P*-lone-pair for interaction with additional metals[51] or, in the application of these compounds in catalysis, possible interaction with substrate molecules.

Compound Mg(Ph$_2$PC{NCy}$_2$)(OAr′)(THF) (**12**) crystallizes as the monomeric compound with a terminal aryloxide ligand

Table 1 Crystal structure and refinement data for [Mg(Ph$_2$PC{NCy}$_2$)Cl(THF)]$_2$ [**6**]$_2$, [Mg(Cy$_2$PC{NCy}$_2$)Br(Et$_2$O)]$_2$ [**7**]$_2$ and [Mg(Cy$_2$PC{N$^i$Pr}$_2$)Cl(THF)]$_2$ [**8**]$_2$

| | [**6**]$_2$ | [**7**]$_2$ | [**8**]$_2$ |
|---|---|---|---|
| Empirical formula | $C_{58}H_{80}N_4O_2Mg_2P_2Cl_2$ | $C_{58}H_{108}N_4O_2Mg_2P_2Br_2$ | $C_{46}H_{88}N_4O_2Mg_2P_2Cl_2$ |
| CCDC Number | 996734 | 996735 | 996736 |
| $M_r$ | 1046.72 | 1163.86 | 910.66 |
| $T$ [K] | 173(2) | 173(2) | 173(2) |
| Crystal size [mm] | 0.25 × 0.20 × 0.15 | 0.20 × 0.20 × 0.20 | 0.15 × 0.10 × 0.05 |
| Crystal system | Triclinic | Triclinic | Monoclinic |
| Space group | $P\bar{1}$ (no. 2) | $P\bar{1}$ (no. 2) | $P2_1/c$ (no. 14) |
| $a$ [Å] | 8.9301(2) | 9.6349(14) | 14.3215(9) |
| $b$ [Å] | 11.0289(3) | 11.1469(9) | 11.5567(7) |
| $c$ [Å] | 16.2637(5) | 16.5610(19) | 15.9545(8) |
| $\alpha$ [°] | 76.778(2) | 88.234(3) | 90 |
| $\beta$ [°] | 84.155(2) | 79.663(4) | 92.786(3) |
| $\gamma$ [°] | 68.586(2) | 67.527(11) | 90 |
| $V$ [Å$^3$] | 1451.39(7) | 1615.5(3) | 2637.5(3) |
| $Z$ | 1 | 1 | 2 |
| $D_{calc.}$ [mg m$^{-3}$] | 1.20 | 1.20 | 1.15 |
| Absorption coefficient [mm$^{-1}$] | 0.23 | 1.36 | 0.25 |
| $\theta$ Range for data collection [°] | 3.59 to 26.02 | 3.59 to 26.73 | 3.47 to 26.02 |
| Reflections collected | 21 660 | 19 523 | 17 706 |
| Independent reflections | 5662 [$R_{int}$ 0.043] | 6791 [$R_{int}$ 0.051] | 5119 [$R_{int}$ 0.106] |
| Reflections with $I > 2\sigma(I)$ | 4710 | 4905 | 3115 |
| Data/restraints/parameters | 5662/0/316 | 6791/112/353 | 5119/0/262 |
| Final $R$ indices [$I > 2\sigma(I)$] | $R_1$ = 0.042, w$R_2$ = 0.102 | $R_1$ = 0.048, w$R_2$ = 0.101 | $R_1$ = 0.072, w$R_2$ = 0.139 |
| Final $R$ indices (all data) | $R_1$ = 0.054, w$R_2$ = 0.108 | $R_1$ = 0.079, w$R_2$ = 0.112 | $R_1$ = 0.134, w$R_2$ = 0.167 |
| GOOF on $F^2$ | 1.039 | 0.998 | 1.015 |
| Largest diff. peak/hole [e Å$^{-3}$] | 0.49 and −0.31 | 0.41 and −0.43 | 0.42 and −0.28 |

**Table 2** Selected bond lengths (Å) and angles (°) for $[\mathbf{6}]_2$, $[\mathbf{7}]_2$ and $[\mathbf{8}]_2$ presented with the corresponding data from $[\mathbf{5}]_2$[23] and $[\mathbf{1}]_2$.[22] All molecules are located on an inversion centre rendering both magnesium atoms equivalent, except for $[\mathbf{5}]_2$; the corresponding parameters for the second magnesium centre are presence in italics. The $\tau_5$-values were calculated according to reference 50

| | $[\mathbf{1}]_2$ [a] | $[\mathbf{5}]_2$ [a] | $[\mathbf{6}]_2$ [b] | $[\mathbf{7}]_2$ [a] | $[\mathbf{8}]_2$ [b] |
|---|---|---|---|---|---|
| Mg–N1 | 2.123(2) | 2.138(2)/*2.119(2)* | 2.1104(16) | 2.071(2) | 2.079(3) |
| Mg–N2 | 2.050(2) | 2.060(2)/*2.060(2)* | 2.0874(16) | 2.108(2) | 2.104(3) |
| Mg–X | 2.5532(9) | 2.7202(9)/*2.7181(9)* | 2.4112(8) | 2.5818(10) | 2.4848(17) |
| Mg–X′ | 2.6789(9) | 2.5364(9)/*2.5406(9)* | 2.4787(8) | 2.6882(10) | 2.4078(16) |
| C1–N1 | 1.331(3) | 1.324(4)/*1.331(3)* | 1.330(2) | 1.341(3) | 1.339(4) |
| C1–N2 | 1.338(3) | 1.333(3)/*1.340(3)* | 1.331(2) | 1.330(3) | 1.325(4) |
| C1–P | — | — | 1.8905(17) | 1.898(3) | 1.889(4) |
| N1–Mg–N2 | 64.76(8) | 64.51(9)/*64.74(9)* | 64.16(6) | 64.27(9) | 63.93(12) |
| N1–Mg–X | 98.32(7) | 161.45(7)/*161.33(7)* | 102.24(5) | 137.56(8) | 98.59(10) |
| N1–Mg–X′ | 165.47(7) | 103.20(8)/*102.08(7)* | 162.56(5) | 99.03(7) | 140.03(11) |
| N2–Mg–X | 123.66(8) | 96.94(7)/*96.78(7)* | 144.36(6) | 100.53(7) | 161.20(11) |
| N2–Mg–X′ | 101.13(7) | 127.94(8)/*132.43(8)* | 99.78(5) | 161.48(7) | 101.55(10) |
| N1–Mg–O | 98.28(9) | 98.84(9)/*99.84(0)* | 100.37(7) | 113.43(10) | 117.09(13) |
| N2–Mg–O | 117.09(10) | 121.64(10)/*118.01(10)* | 112.86(7) | 101.19(10) | 102.62(13) |
| O–Mg–X | 118.43(7) | 90.50(7)/*91.11(7)* | 101.71(6) | 108.25(8) | 91.36(10) |
| O–Mg–X′ | 91.30(7) | 110.00(8)/*109.09(7)* | 92.07(6) | 92.71(7) | 102.10(10) |
| X–Mg–X′ | 86.55(3) | 88.40(3)/*88.36(3)* | 86.97(3) | 86.46(3) | 87.49(5) |
| Mg–X–Mg′ | 93.45(3) | 91.55(3)/*91.69(3)* | 93.03(3) | 93.54(3) | 92.51(5) |
| $\tau_5$ | 0.70 | 0.56/*0.48* | 0.30 | 0.40 | 0.35 |
| $\sum_{\text{angles}}$(P) | — | — | 311.3 | 309.5 | 310.9 |

[a] X = Br. [b] X = Cl.

**Table 3** Crystal structure and refinement data for $Mg(Ph_2PC\{NCy\}_2)(OAr')(THF)$ **12**, $Mg(Ph_2PC\{NCy\}_2)(N\{SiMe_3\}_2)(THF)$ **14** and $Mg(Ph_2PC\{NCy\}_2)(N\{SiMe_3\}_2)(THF)$ **15**

| | **12** | **14** | **15** |
|---|---|---|---|
| Empirical formula | $C_{44}H_{63}N_2O_2MgP$ | $C_{35}H_{58}N_3OMgSi_2P$ | $C_{35}H_{70}N_3OMgSi_2P$ |
| CCDC Number | 996737 | 996738 | 996739 |
| $M_r$ | 707.24 | 648.30 | 660.40 |
| $T$ [K] | 173(2) | 173(2) | 173(2) |
| Crystal size [mm] | 0.30 × 0.30 × 0.25 | 0.25 × 0.25 × 0.20 | 0.28 × 0.22 × 0.16 |
| Crystal system | Monoclinic | Triclinic | Triclinic |
| Space group | $P2_1/c$ (no. 14) | $P\bar{1}$ (no. 2) | $P\bar{1}$ (no. 2) |
| $a$ [Å] | 9.5663(2) | 10.1097(2) | 14.2018(3) |
| $b$ [Å] | 23.8131(5) | 10.4287(2) | 16.0675(3) |
| $c$ [Å] | 18.3412(3) | 19.5149(4) | 18.2651(3) |
| $\alpha$ [°] | 90 | 89.591(1) | 87.827(1) |
| $\beta$ [°] | 95.552(1) | 79.403(1) | 80.418(1) |
| $\gamma$ [°] | 90 | 72.968(1) | 85.172(1) |
| $V$ [Å$^3$] | 4158.58(14) | 1931.30(7) | 4093.92(13) |
| $Z$ | 4 | 2 | 4 |
| $D_{\text{calc.}}$ [mg m$^{-3}$] | 1.13 | 1.12 | 1.07 |
| Absorption coefficient [mm$^{-1}$] | 0.12 | 0.18 | 0.17 |
| $\theta$ Range for data collection [°] | 3.46 to 26.22 | 3.47 to 25.95 | 2.92 to 27.48 |
| Reflections collected | 27 354 | 31 193 | 79 546 |
| Independent reflections | 8147 [$R_{\text{int}}$ 0.059] | 7494 [$R_{\text{int}}$ 0.040] | 18 752 [$R_{\text{int}}$ 0.061] |
| Reflections with $I > 2\sigma(I)$ | 5995 | 6212 | 13 481 |
| Data/restraints/parameters | 8147/0/446 | 7494/0/388 | 18 752/3/788 |
| Final $R$ indices [$I > 2\sigma(I)$] | $R_1$ = 0.061, w$R_2$ = 0.145 | $R_1$ = 0.038, w$R_2$ = 0.089 | $R_1$ = 0.060, w$R_2$ = 0.143 |
| Final $R$ indices (all data) | $R_1$ = 0.087, w$R_2$ = 0.162 | $R_1$ = 0.051, w$R_2$ = 0.095 | $R_1$ = 0.091, w$R_2$ = 0.157 |
| GOOF on $F^2$ | 1.020 | 1.016 | 1.059 |
| Largest diff. peak/hole [e Å$^{-3}$] | 0.44 and −0.44 | 0.29 and −0.23 | 0.84 and −0.94 |

(Tables 3 and 4, Fig. 6); a similar structure was recorded for amidinate **11**.[22] The $\tau_4$-values[52] of 0.67 and 0.63 for **11** and **12**, respectively indicate a geometry closer to tetrahedral than square planar, despite the small bite angle of the ligands (**11** 65.89(9)°, **12** 65.12(8)°). The *N*,*N*′-chelating ligands bond to Mg more symmetrically than in the $[Mg(N\cap N)X(L)]_2$ compounds (max. $\Delta_{MgN}$ 0.023 Å) with equal distribution of π-density across the –NCN– fragment. The terminal aryloxide ligand approaches a linear geometry at oxygen in compound **11** (163.38(18)°) but is considerably more acute in **12** (155.95(16)°)

**Table 4** Selected bond lengths (Å) and angles (°) for **12** presented with the corresponding data from **11**.[22] The $\tau_4$-values were calculated according to ref. 52

| | **11** | **12** |
|---|---|---|
| Mg–N1 | 2.067(2) | 2.062(2) |
| Mg–N2 | 2.054(2) | 2.085(2) |
| Mg–O1 | 1.8431(19) | 1.8463(17) |
| Mg–O2 | 2.005(2) | 2.004(2) |
| C1–N1 | 1.328(3) | 1.328(3) |
| C1–N2 | 1.329(3) | 1.331(3) |
| C1–P | — | 1.892(2) |
| N1–Mg–N2 | 65.89(9) | 65.12(8) |
| N1–Mg–O1 | 134.82(10) | 131.44(9) |
| N1–Mg–O2 | 106.29(9) | 106.76(9) |
| N2–Mg–O1 | 131.25(9) | 139.14(8) |
| N2–Mg–O2 | 111.31(9) | 103.39(9) |
| O1–Mg–O2 | 103.07(9) | 104.58(8) |
| Mg–O1–C$x$[a] | 163.38(18) | 155.95(16) |
| $\tau_4$ | 0.67 | 0.63 |
| $\sum_{\text{angles}}$(P) | — | 312.0 |

[a] **11**, $x$ = 23; **12**, $x$ = 26.

**Table 5** Selected bond lengths (Å) and angles (°) for **14** and **15** presented with the corresponding data from **13**.[22] The $\tau_4$-values were calculated according to ref. 52

| | **13** | **14** | **15**[a] |
|---|---|---|---|
| Mg–N1 | 2.077(2) | 2.0844(14) | 2.084(2)/*2.0681(19)* |
| Mg–N2 | 2.081(2) | 2.0668(14) | 2.0611(19)/*2.059(2)* |
| Mg–N3 | 1.997(2) | 1.9891(14) | 1.992(2)/*1.992(2)* |
| Mg–O | 2.0205(18) | 2.0113(12) | 2.0295(17)/*2.0365(17)* |
| C1–N1 | 1.336(3) | 1.331(2) | 1.337(3)/*1.334(3)* |
| C1–N2 | 1.333(3) | 1.330(2) | 1.335(3)/*1.340(3)* |
| C1–P | — | 1.8910(16) | 1.895(2)/*1.891(2)* |
| N1–Mg–N2 | 65.54(7) | 65.35(5) | 65.20(7)/*65.43(7)* |
| N1–Mg–N3 | 134.26(8) | 132.06(6) | 134.88(8)/*135.98(8)* |
| N1–Mg–O | 108.30(8) | 103.33(6) | 101.08(8)/*99.93(7)* |
| N2–Mg–N3 | 130.83(8) | 130.06(6) | 127.07(8)/*129.91(9)* |
| N2–Mg–O | 106.34(8) | 112.33(5) | 108.61(8)/*110.08(8)* |
| N3–Mg–O | 105.60(8) | 107.24(6) | 111.38(8)/*108.16(8)* |
| Mg–N3–Si1 | 115.41(10) | 117.71(7) | 118.07(11)/*116.95(11)* |
| Mg–N3–Si2 | 117.05(10) | 115.89(8) | 116.25(10)/*117.35(11)* |
| Si1–N3–Si2 | 127.24(12) | 126.27(8) | 125.41(12)/*125.45(12)* |
| $\tau_4$ | 0.67 | 0.69 | 0.70/*0.67* |
| $\sum_{\text{angles}}$(P) | — | 313.6 | 311.7/*311.5* |

[a] Corresponding values for the second molecule in the unit cell presented in *italics*.

despite no apparent adverse steric contacts. Both values fall within the rather large range for aryloxide ligands of this type (146.0(4)°–170.99(9)°).[53,54]

The bis(trimethylsilyl)amide compounds Mg(R$_2$PC{NCy}$_2$)-(N{SiMe$_3$}$_2$)(THF) (**14** R = Ph, **15** R = Cy) both crystallize in the $P\bar{1}$ space group (Tables 3 and 5) but are not isostructural; there are two independent molecules present in the unit cell of **15**. The gross structural features are the same as noted for the amidinate compound **13**,[22] with a chelating [N∩N]$^-$ ligand, terminal amide and coordinated THF (Fig. 7 for **15**; Fig. S3†

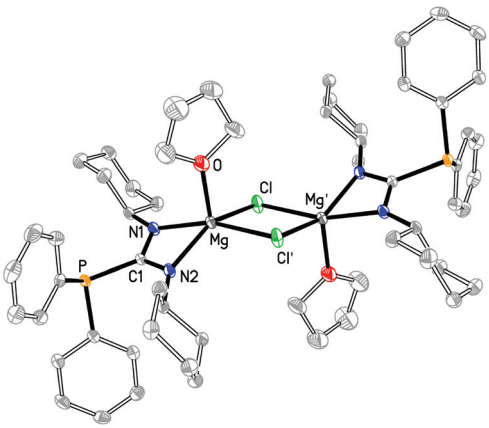


**Fig. 4** Thermal ellipsoid plot (30% probability) of [Mg(Ph$_2$PC{NCy}$_2$)Cl-(THF)]$_2$ [**6**]$_2$ (hydrogen atoms omitted).

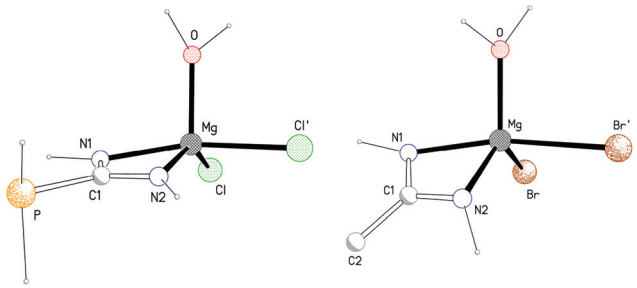


**Fig. 5** Schematic projections of the magnesium environments of [**6**]$_2$ (left) and [**1**]$_2$ (right).

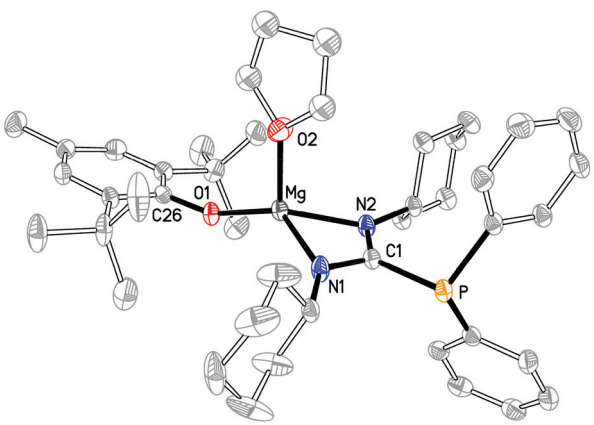


**Fig. 6** Thermal ellipsoid plot (30% probability) of Mg(Ph$_2$PC{NCy}$_2$)-(OAr′)(THF) **12** (hydrogen atoms omitted).

for **14**: see ESI†). The $\tau_4$-values[52] (range 0.67 to 0.70) are similar to those calculated for the aryloxide compounds above, suggesting the bulk of the aryl- and trimethylsilyl-groups is sufficiently removed from the metal environment that little influence is exerted on the metal geometry. The chelating ligands are essentially symmetrically bound (max. $\Delta_{\text{MgN}}$ 0.023 Å), with equal delocalization in the amidine component. The Mg–N$_{\text{amide}}$ distance (range 1.9891(14) Å to 1.992(2) Å) are

 

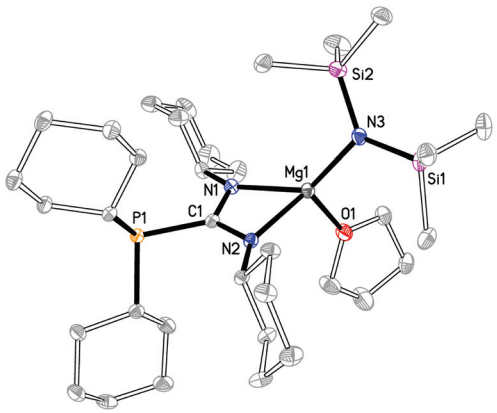


Fig. 7 Thermal ellipsoid plot (30% probability) of one of the independent molecules of $Mg(Cy_2PC\{NCy\}_2)(N\{SiMe_3\}_2)(THF)$ **15** (hydrogen atoms omitted).

typical for terminal amides of this type, and the planar geometry at the nitrogen atoms is as expected.

Although the geometric variations are generally small once a specific structural type has been adopted, the ligand substituents play an important role in determining the gross structure of the compound.[31,55,56] This is illustrated for five structural types observed for the bis(chelate) compounds, $Mg(N\cap N)_2(L)_n$ (Fig. 8). Amidinate compounds **I–III** (Table 6)[31,33,57] represent examples of non-solvated, four coordinate species (Fig. 8a). Each of these compounds was prepared in the presence of THF or $Et_2O$, whereas similar compounds **IV** and **V**,[28,34] were not exposed to donor solvents during their preparation and the structures may therefore not represent the preferred coordination number. Variations of the base-free '$Mg(N\cap N)_2$' unit are seen for bimetallic **VI** and **VII** (Fig. 8b and c).[57] Five-coordinate magnesium centres (Fig. 8d) are adopted for guanidinate (**VIII** and **IX**)[23,27] and amidinate (**X** and **XI**)[23,58] species. In contrast, bis(solvated) compounds (Fig. 8e) are restricted to amidinates **XII–XV**,[23,27,59] including formamidinate compounds **XVI** and **XVII**,[35] where R = H.

Examination of the data in Table 6 shows the C–N–R′ angle ($\alpha$) is largely invariant of structure type and ligand substitution pattern, with most ligands giving values in the range 120°–125°. Exceptions occur when R or R′ = $^t$Bu (**III** and **IV**) or $SiMe_3$ (**X** and **XIII**) for which values tend towards 130°, and for the formamidinate ligands in **XVI** and **XVII** (values generally <120°). The latter correlates well with the reduced size of the R-group and the adoption of a six-coordinate structure. Despite the similar $\alpha$ angles, large variations in the angle between the two metallacycles ($\theta$) exist for compounds with the same structure type. For example, there is only a slight increase in $\alpha$ when the methyl substituent in **I** is replaced with *p*-tolyl in **II**, but a large decrease in $\theta$, and a $\tau_4$-value for **II** consistent with an approximately square-planar metal. Further, the interplay between these parameters is not a direct correlation, as larger $\alpha$ values in compounds **III** and **IV** give greater $\theta$ angles and $\tau_4$-values more fitting for a distorted tetrahedron. The ability of the substituents to interdigitate may play an important role, with significant differences between 'flat' aromatic substituents and more 'spherical' alkyl/silyl groups.

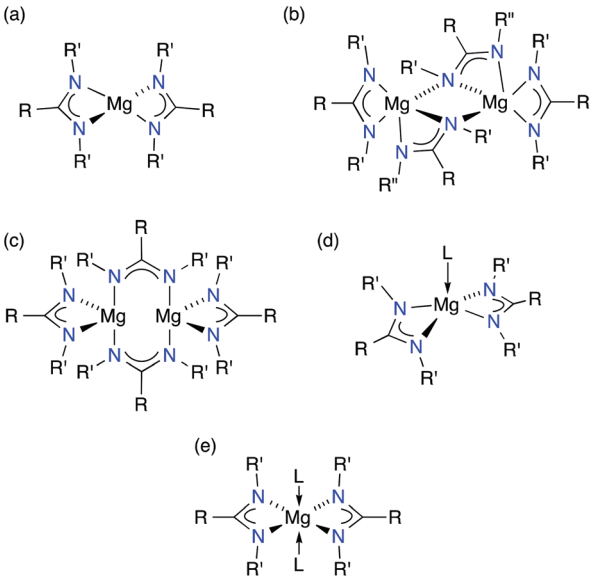


Fig. 8 Different structural types reported for $Mg(N\cap N)_2(L)_n$.

The bis(guanidinate) compounds **VIII** and **IX** are five-coordinate (type 8d). Ignoring electronic contributions to the bonding, this increase in coordination number correlates with the nitrogen of the $-NR''_2$ group removing the R″ substituents from the metal environment. This is supported by the similar $\alpha$ values, and is accentuated by the planar geometry of this nitrogen, which permits rotation such that the substituents are perpendicular to the metallacycle (**VIII** 77.2(5)°; **IX** 79.7(1)° and 80.7(1)°).[60] The six-coordinate compounds **XII** to **XVII** (type 8e) and distorted octahedral with *trans* donor solvent molecules. This enables the metallacycles to be co-planar, maximizing the distance between R′-substituents. The angle $\theta$ is generally small, although the presence of $SiMe_3$ groups in **XIII** causes the ligands to twist relative to each other ($\theta$ = 15.7(2)°).

We conclude, that there is no clear correlation between substituent pattern and structure type for this series of compounds, or for the $[N\cap N]^-$ ligands in general. This unpredictability can be summarized by comparing compounds **III** and **XII** where changing from R′ = $^t$Bu to R′ = $^i$Pr causes an increase in the coordination number from four (type 8a) to six (type 8e).

## Catalysis

Selected examples of compounds described in this work have been examined as (pre)-catalysts for a variety of bond-forming reactions.

**Lactide polymerization.** Magnesium compounds have an established history in promoting the ring-opening polymerization (ROP) of lactide to give poly-lactic acid (PLA). A series of $Mg(N\cap N)X(L)_n$ compounds have been developed based on the β-diketiminate ligand (BDI) system, $[HC\{C(Me)NAr\}_2]^-$, with

**Table 6** Collection of structural parameters for bis(chelate) compounds, $Mg(N\cap N)_2(L)_n$ (see text for references). Structure refers to Fig. 8, $\alpha$ is defined as the C–N–R′ angle, $\theta$ is the inter-planar angle between the two metallacycles (normalized to 0° < $\theta$ < 90°), $\tau$-values are calculated according to ref. 52 ($\tau^4$-) and 50 ($\tau^5$-)

| Coordn no. | Structure | | R | R′/R″ | L | $\alpha$/° | $\theta$/° | $\tau$-value |
|---|---|---|---|---|---|---|---|---|
| 4 | 8a | **I** | Me | Ar[a] | — | 121.2(4) to 122.5(4)[b] | 54.9(2), 54.1(2) | $\tau_4$ = 0.40, 0.41 |
| 4 | 8a | **II** | *p*-tol[c] | Ar[a] | — | 123.8(2), 123.9(2) | 13.3(2) | $\tau_4$ = 0.10 |
| 4 | 8a | **III** | Ph | $^t$Bu | — | 129.5(2), 130.0(2) | 89.8(2) | $\tau_4$ = 0.58 |
| (4)[d] | 8a | **IV** | $^t$Bu | mes[e] | —[d] | 129.7(3), 129.9(3) | 80.3(2) | $\tau_4$ = 0.57 |
| (4)[d] | 8a | **V** | 2,6(mes)$_2$C$_6$H$_3$ | $^i$Pr | —[d] | 128.6(2), 131.2(2) | 88.2(1) | $\tau_4$ = 0.60 |
| 4[f] | 8b | **VI** | Me | Et<br>$^t$Bu | — | 121.4(2), 122.2(2)[g]<br>124.9(2), 125.5(2)[h] | — | — |
| 4[f] | 8c | **VII** | Me | $^i$Pr | — | 121.8(2) | — | — |
| 5 | 8d | **VIII** | N$^i$Pr$_2$ | $^i$Pr | THF | 121.8(7), 122.1(7) | 47.1(5) | $\tau_5$ = 0.57 |
| 5 | 8d | **IX** | N{SiMe$_3$}$_2$ | $^i$Pr | THF | 122.4(2) to 124.5(2)[b] | 44.7(1) | $\tau_5$ = 0.50 |
| 5 | 8d | **X** | Ph | Cy<br>SiMe$_3$ | Et$_2$O | 123.6(3)[i]<br>131.0(3)[j] | 71.3(2) | $\tau_5$ = 0.74 |
| 5 | 8d | **XI** | Mes | Cy | THF | 120.2(1), 121.8(1) | 38.9(1) | $\tau_5$ = 0.41 |
| 6 | 8e | **XII** | Ph | $^i$Pr | THF | 120.6(7), 120.7(6) | 7.4(5) | — |
| 6 | 8e | **XIII** | Ph | SiMe$_3$ | THF | 127.9(3), 130.6(2) | 15.7(2) | — |
| 6 | 8e | **XIV** | C≡CPh | $^i$Pr | THF | 121.0(1), 121.1(1) | 0 | — |
| 6 | 8e | **XV** | *p*-tol[c] | Cy | THF | 121.7(3), 121.8(2) | 0 | — |
| 6 | 8e | **XVI** | H | *p*-tol[c] | THF | 119.0(2) to 122.9(2)[b] | 2.1(1) | — |
| 6 | 8e | **XVII** | H | *o*-tol[k] | THF | 117.4(2), 118.5(2) | 0.2(3) | — |

[a] Ar = 2,6-$^i$Pr$_2$C$_6$H$_3$. [b] Values given as a range. [c] 4-MeC$_6$H$_4$. [d] Prepared in the absence of coordinating solvent. [e] 2,4,6-Me$_3$C$_6$H$_2$. [f] $\alpha$ values reported for chelating ligands only. [g] Angle to Et-substituent. [h] Angle to $^t$Bu-substituent. [i] Angle to Cy-substituent. [j] Angle to SiMe$_3$-substituent. [k] 2-MeC$_6$H$_4$.

X = alkyl,[61–63] amide,[63–66] or alkoxide.[64,67–69] Accordingly we examined selected compounds to assess their behaviour as ROP catalysts.

Phosphaguanidinate compounds **6**, **8**, **12** and **14** were initially screened for activity on an NMR scale with 20 equivalents of *rac*-lactide. The chlorides **6** and **8** were inactive at room temperature and 70 °C, consistent with the requirement of a reactive Mg–X bond (where X = alkyl, amide, alkoxide) to initiate polymerization. The aryloxide **12** did not show appreciable activity at room temperature, but was active at 70 °C, giving a conversion of <95% after 6 h. This is consistent with a slow initiation due to the large aromatic substituent of the aryloxide.

The amide **14** was considerably more active, with <95% conversion after 30 min at room temperature. The $^1$H NMR spectra of this reaction showed non-coordinated THF, and a shift of Si*Me*$_3$ resonances to −0.03 ppm, which is inconsistent with the liberation of HN{SiMe$_3$}$_2$ ($\delta_H$ 0.09 in C$_6$D$_6$). However, the $^{31}$P{$^1$H} NMR spectra showed that polymerization initiated by **12** and **14** proceed with loss of the phosphaguanidine, Ph$_2$PC{NCy}{NHCy}, identified by a characteristic singlet at $\delta_P$ −16.9.[24]

Amidinate- and guanidinate-amides (**13** and **16**) were also tested. Both compounds promoted the NMR scale polymerization at room temperature, with <95% conversion after 2 h (**13**) and 5 minutes (**16**). The rapid polymerization promoted by the hpp-derivative **16** is consistent with the lack of a coordinating solvent that would compete with the monomer for access to the metal.[70] However, in both cases the non-coordinated ligand was identified in solution by $^1$H NMR spectroscopy, consistent with rapid loss of the *N*,*N*′-chelate.

Whilst these compounds demonstrate good activity for the polymerization of lactide, their development as useful reagents is limited, with any control of polymerization imparted by the *N*,*N*-chelate lost on conversion to the active species. In addition, the neutral compound hppH is an excellent organocatalyst for lactide polymerization (1 mol% hppH gives 99% conversion of L-lactide in 20 seconds),[71] and the observed polymerization activity of **16** may therefore be due to the presence of liberated guanidine.

**Dimerization of aldehydes (the Tishchenko reaction).** In 2007 Hill and co-workers rekindled research in the homocoupling of aldehydes promoted by main group elements other than aluminium.[72] They examined the catalytic activity of amide compounds of Ca, Sr and Ba, initially supported by the BDI ligand. Subsequent work with main group elements includes compounds of Li,[73,74] Na,[73,75,76] K,[73] and most recently Zn.[77] Magnesium reagents have been used in the presence of thiolate[18,19,78] and selenide anions[79] to promote this coupling reaction. We have previously communicated our work in this area with amidinate compounds **11** and **13**,[22] and guanidinates **16** and **17**.[21] We report here the catalytic performance of the phosphaguanidinate amides **14** and **15**.

The esterification of benzaldehyde was examined on an NMR scale in C$_6$D$_6$ using 1 mol% of **14** and **15** with 1,4-dimethoxybenzene as an internal standard. During the initial 10 minutes, compounds **14** and **15** produce 60% and 46% yields of benzylbenzoate, respectively (Fig. 9), corresponding to turnover frequencies (TOFs) of 360 h$^{-1}$ (**14**) and 276 h$^{-1}$ (**15**). This represents a marked increase in the rate of reaction over the same time period when compared with **13** (yield 37%, TOF ~ 220 h$^{-1}$) and **16**/**17** (yields ~20%, TOFs ~ 120 h$^{-1}$). The rate

 

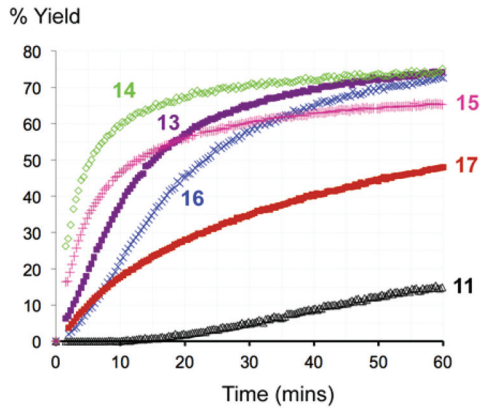


Fig. 9 Graphical representation of the activity of magnesium amide and aryloxide compounds for the catalytic dimerization of benzaldehyde.

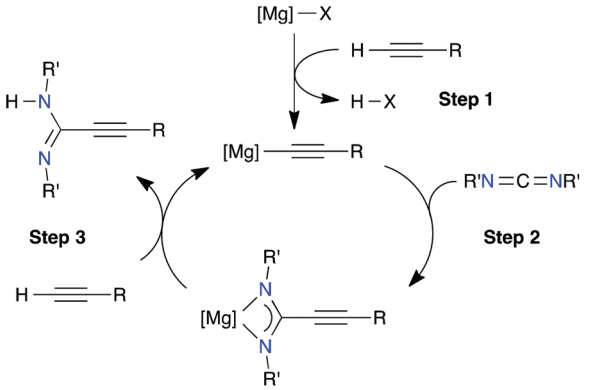


Scheme 5 [Mg] = 'Mg(mesC{NCy}$_2$)', solvent omitted.

of ester production decreases after this time [30 minutes: 70% (**14**), 60% (**15**); 60 minutes: 74% (**14**), 65% (**15**)], likely due to the reduced concentration of substrate in the closed system.

In contrast to the lactide polymerization catalysis, $^{31}P\{^1H\}$ NMR analysis of the reaction mixtures showed no liberated phosphaguanidine, suggesting that the ligand remains associated with the magnesium during the catalysis. The GCMS trace of a hydrolysed reaction between **15** with two equivalents of benzaldehyde shows the expected organic species PhC(O)H, $PhCH_2OH$, $PhC(O)N\{SiMe_3\}_2$ and $PhC(O)OCH_2Ph$, in addition to the silyl exchange products $PhCH_2OSiMe_3$ and $PhC(O)NHSiMe_3$.[21] Peaks for $PCy_2H$ and CyN=C=NCy are also observed, but believed to be due to the facile cleavage of the P–C bond during sample preparation.[80]

**Hydroacetylenation of carbodiimides.** Ethynylamidines, RC≡CC{NR′}{NHR′}, are potentially valuable building blocks to organic compounds containing more complex heterocycles including isoxazoles and pyrazoles.[81–83] Although the preparation of the metal-bound amidinates *via* the insertion of a carbodiimide into a terminal metal–acetylide bond is facile, hydrolysis to liberate the free amidine is not viable due to the sensitivity of the products to these conditions.[84] This has led to research into the catalytic production of these unsaturated molecules,[85] with most work to date focussed on the lanthanide elements.[84,86,87]

The use of main group compounds as catalysts was first reported in 2006 using commercially available $LiN\{SiMe_3\}_2$.[88] Subsequently, Hill and co-workers studied the stoichiometric insertion of carbodiimides into Ca–C bonds of BDI-supported acetylide compounds.[89] Despite observing catalytic turnover at 80 °C in toluene, loss of the BDI-ligand was detected by NMR spectroscopy. Building on these results, Hill's team has reported catalytic hydroacetylenation of carbodiimides using the solvated homoleptic amides, $M(N\{SiMe_3\}_2)_2(THF)_2$ (M = Mg, Ca, Sr).[90] These simple catalysts show high activities and demonstrate improved substrate scope by extending the coupling to include bulky carbodiimide derivatives (*e.g.* R′ = 2,6-$^i$Pr$_2$C$_6$H$_3$).

We reported the hydroacetylenation of carbodiimides using compound **13**, with an NMR yield of 72% after 24 h at 80 °C.[23] Subsequent investigations using bis(chelate) compounds **2**, **9** and **10** showed similar activities (range 72%–74%) demonstrating that the amide was not a requirement for catalysis. Indeed, catalytic turnover was also observed for organometallic and organoamide compounds of magnesium, including Grignard reagents RMgX. This demonstrated multiple entry points into the accepted catalytic cycle (Scheme 5), prompting further investigation through stoichiometric reactions.

The procedure for NMR scale catalysis involves the addition of the magnesium reagent to a pre-mixed, equimolar solution of the alkyne and the carbodiimide. For **13**, it is assumed the reaction proceeds *via* protonolysis of the amide and formation of the terminal acetylide (**Step 1**, Scheme 5). However, insertion of carbodiimide into the Mg–N bond to form a guanidinate ligand is a viable alternative pathway (see Scheme 1). A competition reaction performed using a 1 : 1 : 1 ratio of [**13**]: $^i$PrN=C=N$^i$Pr : PhC≡CH in $C_6D_6$, showed that both pathways operate under these conditions. The $^1$H NMR spectrum showed $HN\{SiMe_3\}_2$ (from **Step 1**) and $\{Me_3Si\}_2NC\{N^iPr\}\{NH^iPr\}$ (**I**, Scheme 6), which originates from carbodiimide insertion to form amidinate/guanidinate species **B** prior to protonation by phenylacetylene. The relative ratio of $HN\{SiMe_3\}_2$ : **I**, calculated from $^1$H NMR integrals of the Si*Me*$_3$ peaks, was 9 : 1 showing that **Step 1** dominates the reactivity.

The insertion of the carbodiimide into the Mg–C bond (**Step 2**, Scheme 5) is generally considered an irreversible step. To examine this, 1 equiv. of $^i$PrN=C=N$^i$Pr was added to **A** (generated *in situ*), to form the heteroleptic bis(amidinate) species **C** containing the $[PhC{\equiv}CC\{N^iPr\}_2]^-$ ligand. Subsequent addition of 1 equiv. CyN=C=NCy did not show formation the corresponding *N*,*N*-dicyclohexyl-2-phenylethynylamidinate compound. Given the similar reactivity of the two carbodiimides during catalysis,[23] this suggests that 'de-insertion' of *N*,*N*′-diisopropylcarbodiimide does not occur to an appreciable extent. Although previous studies showed that **C** undergoes ligand re-distribution to form the homoleptic bis(amidinate)s **9** and **10**, the lack of CyN=C=NCy incorpor-

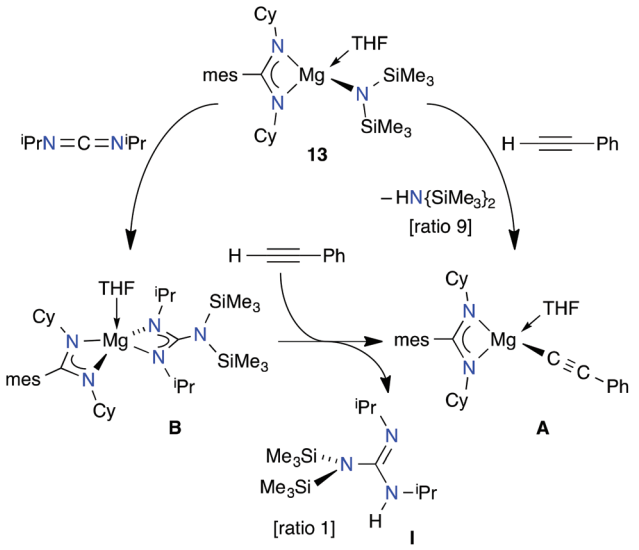


Scheme 6

ated into the system is good evidence that formation of the amidinate ligands is essentially an irreversible process.

The relative protolytic stability of the amidinate and guanidinate ligands generated during the catalysis initiated by **13** is important in determining the mechanism. Experiments show that the amidinate ligand, $[mesC\{NCy\}_2]^-$, is relatively resistant to protonolysis when compared with $[\{Me_3Si\}_2NC\{N^iPr\}_2]^-$ and $[PhC{\equiv}CC\{N^iPr\}_2]^-$. For example, no reaction was observed upon heating NMR samples bis(amidinate)s **9** or **10** to 80 °C in the presence of 5 equivalents of phenylacetylene, whereas the bis(guanidinate) **2** quantitatively liberates guanidine **I** under these conditions. This contradicts the observation that bis(amidinate) **10** is active in hydroacetylenation and highlights the limitations of comparing the results of stoichiometric reactions with the complex equilibria present during a catalytic experiment. As noted for Hill's strontium system,[90] there was a negligible kinetic isotope effect when the catalysis was performed with deuterated phenylacetylene (Fig. S5†) suggesting that the protonation of the amidinate by phenylacetylene is not involved in the rate determining step.

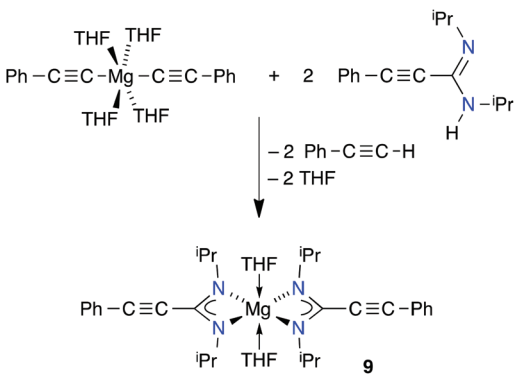


Scheme 7

Hill reports that catalysis initiated by the group 2 bis(amide) compounds is subject to a significant product inhibition effect. Kinetic analysis of the Sr case suggested that this proceeded by competitive protonolysis of the metal amidinate by the amidine product rather than the phenylacetylene.[90] To investigate whether this process was operating in our system, the stoichiometric reaction between $Mg(C{\equiv}CPh)_2(THF)_4$ and ethynylamidine $PhC{\equiv}CC\{N^iPr\}\{NH^iPr\}$, was performed (Scheme 7). Quantitative formation of the bis(amidinate) **9** with formation of phenylacetylene indicates that the terminal magnesium acetylide ligand is susceptible to protonolysis by the amidine product, and suggests that **Step 3** may be reversible.

## Conclusions

We have demonstrated that amidinate, guanidinate and phosphaguanidinate compounds of magnesium are accessible through standard synthetic procedures. The insertion of carbodiimides into Mg–C and Mg–N bonds is an efficient route to amidinate and guanidinate compounds, respectively, whereas protonation of organomagnesium groups was the preferred route to phosphaguanidinate compounds. The substitution pattern of the ligand may influence the constitution of the species isolated from the reaction, with ligand redistribution a possibility in solution. Surveying a range of compounds from the literature failed to identify a single structural parameter that correlated with the type of solid-state structure adopted, although the ability of the ligand substituents to pack efficiently around the small magnesium centre is believed to play an important role.

Selected compounds show good activity in a range of bond-forming catalytic reactions. However, the extent to which the integrity of the metal reagent is maintained during catalysis has been questioned. In the case of the ring-opening polymerization of lactide, the loss of the ligand from magnesium was confirmed and so it was concluded that these species were of limited use.

Although loss of the ligand from the metal was not observed for the dimerization of aldehydes, the factors that control the activity remain unclear. Thus the reason for the increased activity observed for the phosphaguanidinate compounds is not well understood, but must result from the presence of the terminal $-PR_2$ groups. Finally, stoichiometric studies have shown that the hydroacetylenation catalysis is dominated by the presence of multiple equilibria in solution and that, provided a polar organomagnesium or magnesium-amide bond is present at some point during the catalytic cycle, access to active species is achieved with little loss to activity. So, although the ligands presented in this study have enabled some interesting chemistry to be explored, we regretfully conclude that their future development in the areas of catalysis presented in this contribution is, at best questionable. Pathway 1 in Scheme 8 may be playing a more dominant role in magnesium-based catalysis than we first assumed.

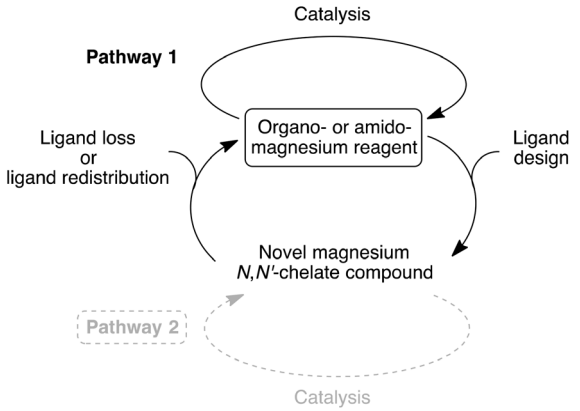


Scheme 8

## Acknowledgements

Victoria Master's by thesis Scholarship (RJS).

## Notes and references

1 M. Arrowsmith and M. S. Hill, in *Comprehensive Inorganic Chemistry II*, ed. T. Chivers, Elsevier, 2013, vol. 1, pp. 1189–1216.
2 M. R. Crimmin and M. S. Hill, in *Topics in Organometallic Chemistry*, ed. S. Harder, 2013, pp. 191–241.
3 A. G. M. Barrett, M. R. Crimmin, M. S. Hill and P. A. Procopiou, *Proc. R. Soc. London, Ser. A*, 2010, **466**, 927–963.
4 S. Harder, *Chem. Rev.*, 2010, **110**, 3852–3876.
5 X. Zhang, T. J. Emge and K. C. Hultzsch, *Angew. Chem., Int. Ed.*, 2012, **51**, 394–398.
6 M. Arrowsmith, M. R. Crimmin, A. G. M. Barrett, M. S. Hill, G. Kociok-Köhn and P. A. Procopiou, *Organometallics*, 2011, **30**, 1493–1506.
7 S. R. Neal, A. Ellern and A. D. Sadow, *J. Organomet. Chem.*, 2011, **696**, 228–234.
8 J. F. Dunne, D. B. Fulton, A. Ellern and A. D. Sadow, *J. Am. Chem. Soc.*, 2010, **132**, 17680–17683.
9 M. R. Crimmin, M. Arrowsmith, A. G. M. Barrett, I. J. Casely, M. S. Hill and P. A. Procopiou, *J. Am. Chem. Soc.*, 2009, **131**, 9670–9685.
10 D. Mukherjee, A. Ellern and A. D. Sadow, *Chem. Sci.*, 2014, **5**, 959–964.
11 M. Arrowsmith, M. S. Hill and G. Kociok-Köhn, *Chem. – Eur. J.*, 2013, **19**, 2776–2783.
12 M. Arrowsmith, T. J. Hadlington, M. S. Hill and G. Kociok-Köhn, *Chem. Commun.*, 2012, **48**, 4567–4569.
13 M. Arrowsmith, M. S. Hill, T. J. Hadlington and G. Kociok-Köhn, *Organometallics*, 2011, **30**, 5556–5559.
14 J. F. Dunne, S. R. Neal, J. Engelkemier, A. Ellern and A. D. Sadow, *J. Am. Chem. Soc.*, 2011, **133**, 16782–16785.
15 W. Yi and H. Ma, *Dalton Trans.*, 2014, **43**, 5200–5210.
16 H.-J. Chuang, H.-L. Chen, J.-L. Ye, Z.-Y. Chen, P.-L. Huang, T.-T. Liao, T.-E. Tsai and C.-C. Lin, *J. Polym. Sci., Part A: Polym. Chem.*, 2013, **51**, 696–707.
17 Y. Wang, W. Zhao, X. Liu, D. Cui and E. Y.-X. Chen, *Macromolecules*, 2012, **45**, 6957–6965.
18 S. P. Curran and S. J. Connon, *Angew. Chem., Int. Ed.*, 2012, **51**, 10866–10870.
19 L. Cronin, F. Manoni, C. J. O'Connor and S. J. Connon, *Angew. Chem., Int. Ed.*, 2010, **49**, 3045–3048.
20 W. Tischtschenko, *Chem. Zentralbl.*, 1906, **77**, 1309.
21 B. M. Day, N. E. Mansfield, M. P. Coles and P. B. Hitchcock, *Chem. Commun.*, 2011, **47**, 4995–4997.
22 B. M. Day, W. Knowelden and M. P. Coles, *Dalton Trans.*, 2012, **41**, 10930–10933.
23 R. J. Schwamm and M. P. Coles, *Organometallics*, 2013, **32**, 5277–5280.
24 J. Grundy, M. P. Coles and P. B. Hitchcock, *Dalton Trans.*, 2003, 2573–2577.
25 N. E. Mansfield, J. Grundy, M. P. Coles, A. G. Avent and P. B. Hitchcock, *J. Am. Chem. Soc.*, 2006, **128**, 13879–13893.
26 G. M. Sheldrick, *SHELXL-97, Program for the Refinement of Crystal Structures*, Göttingen, 1997.
27 B. Srinivas, C.-C. Chang, C.-H. Chen, M. Y. Chiang, I.-T. Chen, Y. Wang and G.-H. Lee, *J. Chem. Soc., Dalton Trans.*, 1997, 957–963.
28 J. A. R. Schmidt and J. Arnold, *J. Chem. Soc., Dalton Trans.*, 2002, 2890–2899.
29 M.-D. Li, C.-C. Chang, Y. Wang and G.-H. Lee, *Organometallics*, 1996, **15**, 2571–2574.
30 O. Ciobanu, A. Fuchs, M. Reinmuth, A. Lebkücher, E. Kaifer, H. Wadepohl and H.-J. Himmel, *Z. Anorg. Allg. Chem.*, 2010, **636**, 543–550.
31 N. Nimitsiriwat, V. C. Gibson, E. L. Marshall, P. Takolpuckdee, A. K. Tomov, A. J. P. White, D. J. Williams, M. R. J. Elsegood and S. H. Dale, *Inorg. Chem.*, 2007, **46**, 9988–9997.
32 S. P. Green, C. Jones and A. Stasch, *Science*, 2007, **318**, 1754–1757.
33 R. T. Boeré, M. L. Cole and P. C. Junk, *New J. Chem.*, 2005, **29**, 128–134.
34 A. Xia, H. M. El-Kaderi, M. J. Heeg and C. H. Winter, *J. Organomet. Chem.*, 2003, **682**, 224–232.
35 M. L. Cole, D. J. Evans, P. C. Junk and L. M. Louis, *New J. Chem.*, 2002, **26**, 1015–1024.
36 F. A. Cotton, S. C. Haefner, J. H. Matonic, X. Wang and C. A. Murillo, *Polyhedron*, 1997, **16**, 541–550.
37 M. P. Coles, *Chem. Commun.*, 2009, 3659–3676.
38 M. R. Crimmin, A. G. M. Barrett, M. S. Hill, P. B. Hitchcock and P. A. Procopiou, *Organometallics*, 2008, **27**, 497–499.
39 A. G. M. Barrett, M. R. Crimmin, M. S. Hill, P. B. Hitchcock, S. L. Lomas, M. F. Mahon and P. A. Procopiou, *Dalton Trans.*, 2010, **39**, 7393–7400.
40 T. M. A. Al-Shboul, G. Volland, H. Görls and M. Westerhausen, *Z. Anorg. Allg. Chem.*, 2009, **635**, 1568–1572.

41 B. M. Day and M. P. Coles, *Eur. J. Inorg. Chem.*, 2010, 5471–5477.
42 A. C. Behrle and J. A. R. Schmidt, *Organometallics*, 2013, **32**, 1141–1149.
43 A. J. Roering, S. E. Leshinski, S. M. Chan, T. Shalumova, S. N. MacMillan, J. M. Tanski and R. Waterman, *Organometallics*, 2010, **29**, 2557–2565.
44 N. E. Mansfield, J. Grundy, M. P. Coles and P. B. Hitchcock, *Polyhedron*, 2010, **29**, 2481–2488.
45 W.-X. Zhang, M. Nishiura, T. Mashikp and Z. Hou, *Chem. – Eur. J.*, 2008, **14**, 2167–2179.
46 N. E. Mansfield, M. P. Coles and P. B. Hitchcock, *Dalton Trans.*, 2005, 2833–2841.
47 M. P. Coles and P. B. Hitchcock, *Chem. Commun.*, 2002, 2794–2795.
48 P. C. Andrews, M. Brym, C. Jones, P. C. Junk and M. Kloth, *Inorg. Chim. Acta*, 2006, **359**, 355–363.
49 J. Cheng, *Acta Crystallogr., Sect. E: Struct. Rep. Online*, 2011, **67**, m987.
50 A. W. Addison, T. N. Rao, J. Reedijk, J. van Rijn and G. C. Verschoor, *J. Chem. Soc., Dalton Trans.*, 1984, 1349–1356.
51 J. Grundy, N. E. Mansfield, M. P. Coles and P. B. Hitchcock, *Inorg. Chem.*, 2008, **47**, 2258–2260.
52 L. Yang, D. R. Powell and R. P. Houser, *Dalton Trans.*, 2007, 955–964.
53 A. D. Pajerski, E. P. Squiller, M. Parvez, R. R. Whittle and H. G. Richey Jr., *Organometallics*, 2005, **24**, 809–814.
54 K. W. Henderson, G. W. Honeyman, A. R. Kennedy, R. E. Mulvey, J. A. Parkinson and D. C. Sherrington, *Dalton Trans.*, 2003, 1365–1372.
55 M. P. Coles, D. C. Swenson, R. F. Jordan and V. G. Young Jr., *Organometallics*, 1997, **16**, 5183–5194.
56 M. P. Coles, D. C. Swenson, R. F. Jordan and V. G. Young Jr., *Organometallics*, 1998, **17**, 4042–4048.
57 A. R. Sadique, M. J. Heeg and C. H. Winter, *Inorg. Chem.*, 2001, **40**, 6349–6355.
58 M. Fan, Q. Yang, H. Tong, S. Yuan, B. Jia, D. Guo, M. Zhou and D. Liu, *RSC Adv.*, 2012, **2**, 6599–6605.
59 D. Walther, P. Gebhardt, R. Fischer, U. Kreher and H. Görls, *Inorg. Chim. Acta*, 1998, **281**, 181–189.
60 S. L. Aeilts, M. P. Coles, D. C. Swenson, R. F. Jordan and V. G. Young Jr., *Organometallics*, 1998, **17**, 3265–3270.
61 M. H. Chisholm, K. Choojun, J. C. Gallucci and P. M. Wambua, *Chem. Sci.*, 2012, **3**, 3445–3457.
62 C. N. Ayala, M. H. Chisholm, J. C. Gallucci and C. Krempner, *Dalton Trans.*, 2009, 9237–9245.
63 X. Xu, Y. Chen, G. Zou, Z. Ma and G. Li, *J. Organomet. Chem.*, 2010, **695**, 1155–1162.
64 M. H. Chisholm, J. C. Gallucci and K. Phomphrai, *Inorg. Chem.*, 2002, **41**, 2785–2794.
65 M. H. Chisholm and K. Phomphrai, *Inorg. Chim. Acta*, 2003, **350**, 121–125.
66 A. P. Dove, V. C. Gibson, E. L. Marshall, A. J. P. White and D. J. Williams, *Dalton Trans.*, 2004, 570–578.
67 M. H. Chisholm, J. C. Huffman and K. Phomphrai, *J. Chem. Soc., Dalton Trans.*, 2001, 222–224.
68 B. M. Chamberlain, M. Cheng, D. R. Moore, T. M. Ovitt, E. B. Lobovsky and G. W. Coates, *J. Am. Chem. Soc.*, 2001, **123**, 3229–3238.
69 F. Drouin, T. J. J. Whitehorne and F. Schaper, *Dalton Trans.*, 2011, **40**, 1396–1400.
70 M. P. Coles and P. B. Hitchcock, *Eur. J. Inorg. Chem.*, 2004, 2662–2672.
71 R. C. Pratt, B. G. G. Lohmeijer, D. A. Long, R. M. Waymouth and J. L. Hedrick, *J. Am. Chem. Soc.*, 2006, **128**, 4556–4557.
72 M. R. Crimmin, A. G. M. Barrett, M. S. Hill and P. A. Procopiou, *Org. Lett.*, 2007, **9**, 331–333.
73 K. Rajesh and H. Berke, *Adv. Synth. Catal.*, 2013, **355**, 901–906.
74 M. M. Mojtahedi, E. Akbarzadeh, R. Sharifi and M. S. Abaee, *Org. Lett.*, 2007, **9**, 2791–2793.
75 T. Werner and J. Koch, *Eur. J. Org. Chem.*, 2010, 6904–6907.
76 D. C. Waddell and J. Mack, *Green Chem.*, 2009, **11**, 79–82.
77 J. Li, J. Shi, H. Han, G. Z. H. Tong, X. Wei, D. Liu and M. F. Lappert, *Organometallics*, 2013, **32**, 3721–3727.
78 C. J. O'Connor, F. Manoni, S. P. Curran and S. J. Connon, *New J. Chem.*, 2011, **35**, 551–553.
79 S. P. Curran and S. J. Connon, *Org. Lett.*, 2012, **14**, 1074–1077.
80 N. E. Mansfield, M. P. Coles and P. B. Hitchcock, *Polyhedron*, 2012, **37**, 9–13.
81 G. Himbert, W. Schwickerath and G. Maas, *Liebigs Ann. Chem.*, 1985, 1389–1397.
82 G. Himbert and W. Schwickerath, *Liebigs Ann. Chem.*, 1984, 85–97.
83 H. Fujita, R. Endo, A. Aoyama and T. Ichii, *Bull. Chem. Soc. Jpn.*, 1972, **45**, 1846.
84 W.-X. Zhang, M. Nishiura and Z. Hou, *J. Am. Chem. Soc.*, 2005, **127**, 16788–16789.
85 W.-X. Zhang and Z. Hou, *Org. Biomol. Chem.*, 2008, **6**, 1720–1730.
86 W. Yi, J. Zhang, M.-D. Li, Z. Chen and X. Zhou, *Inorg. Chem.*, 2011, **50**, 11813–11824.
87 L. Xu, Y.-C. Wang, W.-X. Zhang and Z. Xi, *Dalton Trans.*, 2013, **42**, 16466–16469.
88 T.-G. Ong, J. S. O'Brien, I. Korobkov and D. S. Richeson, *Organometallics*, 2006, **25**, 4728–4730.
89 A. G. M. Barrett, M. R. Crimmin, M. S. Hill, P. B. Hitchcock, S. L. Lomas, M. F. Mahon, P. A. Procopiou and K. Suntharalingam, *Organometallics*, 2008, **27**, 6300–6306.
90 M. Arrowsmith, M. R. Crimmin, M. S. Hill, S. L. Lomas, M. S. Heng, P. B. Hitchcock and G. Kociok-Köhn, *Dalton Trans.*, 2014, **43**, DOI: 10.1039/c3dt53542h.